Predictability of seasonal East Coast winter storm surge impacts

with application to New York's Long Island

(Running Title: Predictability of East Coast winter storm surge impacts)

Arthur T. DeGaetano

Northeast Regional Climate Center

Department of Earth and Atmospheric Sciences

Cornell University

Ithaca, NY

Submitted to *Meteorological Applications*

July, 2007

Keywords: Seasonal prediction, winter storms, tidal surge, United States

Corresponding author address:

Dr. Art DeGaetano, 1119 Bradfield Hall,

Cornell University, Ithaca, NY 14850

Email: atd2@cornell.edu

Abstract

The characteristics of seasons with enhanced East Coast winter storm and storm surge activity are identified from among a set of global atmospheric circulation indices and local land and sea surface temperature anomalies. Without regard for storm strength or surge potential, the most active East Coast winter storm (ECWS) seasons occur in association with El Niño events. There is also some indication that such seasons are preferred under the positive phase of the Pacific decadal oscillation. In terms of storm surge potential, forecasts of strong ECWS activity are more skillful than direct forecasts of the number of extreme surge events. In both cases, sea surface temperatures (SST) off the southeast U.S. coast and in the Gulf of Mexico differentiate high seasonal activity from relatively inactive seasons. Warmer than normal SST in both regions during summer provide a measure of storm activity in the subsequent winter.

The results provide a means of anticipating seasonal East Coast winter storm activity, and to some degree impacts, that is similar to widely used forecasts of tropical storm activity. From a predictive standpoint, forecasts of active strong storm seasons and low surge activity exhibit fairly high false alarm ratios. However, the false alarm rate for forecasts of low storm activity or high surge activity is less than 10%.

1. Introduction

Coastal interests in the Northeastern United States are particularly vulnerable to impacts related to East Coast winter storms (ECWS). In fact, it can be argued that the adverse effects of these storms exceed those of hurricanes along the metropolitan Northeast coastline, given their higher frequency of occurrence and more widespread impacts. A cursory examination of the publication *Storm Data* supports this claim. During the late 1990s, ECWS resulted in 5 deaths and over 30 injuries in the New York Metropolitan Area (defined as coastal New York and New Jersey). Comparatively, tropical weather systems resulted in only one death and four injuries. In terms of economic losses, ECWS were responsible for nearly 50 million dollars in damage, compared to 2 million in tropical cyclone loses. Leatherman (1982) cites coastal storms (both extratropical and tropical) as a major contributor to beach and dune erosion, overwash processes and the opening of tidal inlets on barrier islands.

Many of the coastal impacts of ECWS result from the larger spatial dimensions and longer durations of these storms relative to hurricanes. ECWS tend to persist over numerous tidal cycles and thus their potential to produce coastal impacts from high winds, waves and increased water levels extends over days rather than hours. Likewise, the winds from these storms are able to trap ebb tidal flow in areas away from the immediate coast (e.g. within Long Island Sound) allowing water levels to build over several tidal cycles.

Despite the severity of the economic, environmental and societal impacts resulting from ECWS, little is known about their climatological variability or the influence that other large scale events and components of the global atmosphere and oceans exert on their frequency and severity. The climatology of ECWS has been examined by Mather *et al*. (1964) based on documentary accounts; Davis *et al*. (1993) using wave heights; and Hirsch *et al*. (2001) based on the NCEP/NCAR Reanalysis data set (Kalnay *et al*., 1996). Hirsch *et al*. (2001) found average monthly ECWS frequency anomalies to be significantly higher during El Niño months when compared to neutral months over the October-April storm season. ECWS show little or no change in frequency anomalies during La Niña months.

DeGaetano *et al*. (2002) and Chan *et al*. (2003) extended these results through empirical analyses of the relationship between ECWS activity and various atmospheric indices. DeGaetano *et al*. (2002) showed that sea surface temperatures in the Gulf of Mexico during the previous storm season provided a measure of ECWS activity during the subsequent December through February period. Warmer than normal Gulf temperatures were typically associated with active seasons. It was shown that this variable was related to both El Niño and North Atlantic Oscillation (NAO) phase, as heightened storm activity tended to occur during the positive phase of the NAO and El Niño conditions. Over a longer October –April storm season, high activity tended to be associated with warmer than normal sea surface temperature off the Southeast U.S. coast during the preceding summer.

Chan *et al*. (2003) compared 500 hPa height anomalies between active and inactive ECWS seasons. An October dipole, with stronger than normal 500 hPa geostrophic westerlies over the eastern Pacific, was associated with higher than average storm activity from November through April. Such seasons were also characterized by weaker than average 500 hPa geostrophic westerlies over the North Atlantic. These relationships tended to be modulated by the phase of the El Niño Southern Oscillation.

In the current work, these results are extended by focusing on a subset of storms that are most likely to produce coastal flooding and erosion impacts on New York's Long Island. This portion of the Northeast coast provides the focus of the study based on stakeholder (emergency managers and coastal engineers) interest in anticipating seasonal storm impacts; the extensive south-facing coastline of the Island, and the high potential for economic and environmental impacts. In section 2 the use of tide gauge data to isolate impact-producing ECWS events is discussed. Likewise, an alternative definition of seasonal ECWS activity based on tidal surge rather than meteorological parameters is introduced. In section three, a refined statistical methodology is described. Results, both in terms of diagnostic and predictive meteorological variables, are presented in section 4.

2. Data

2.1. Seasonal storm counts

The methods of Hirsch *et al.* (2001) were used to identify ECWS. By definition, ECWS were required to be located within the quadrilateral bounded at 45° N latitude by 65° W and 70° W longitude and at 30° N latitude by 75° W and 85° W longitude. A slight modification was incorporated into the original objective identification algorithm, expanding the range of valid tracks to include storms with a motion from 270° to 90°. Originally, some northward component of storm motion was required. However, when compared to surge records, it became apparent that several noteworthy storms were excluded by this criterion. Overall, the effect of this change was to increase the average number of storms per season by more than 30%. However, the correlation between the two series was high (r = 0.86).

Subsets of storms were defined based on the magnitude of storm surge observed at tide gauges along and adjacent to the southern shore of New York's Long Island. Hourly values of observed and predicted tides were obtained from the NOAA Center for Operational Oceanographic Products and Services (CO-OPS) website http://tidesandcurrents.noaa.gov/. Long-term data were available from four sites in the New York City metropolitan region. Data from Montauk (station 8510560), The Battery (station 8518750) and Sandy Hook, NJ (station 8531680) were available from 1959-2005. Data at Willets Point (station 8516990) were discontinued in 1999.

All data were with respect to the mean lower-low water level and were adjusted prior to 1983 to account for the epoch adjustment. In practice, tides are referenced with regard to a specific 19-year period or epoch, the most recent spanning the period 1983-2001. The recomputed epoch accounts for astronomical, anthropogenic and geological variations in tidal levels through the period (Hess, 2003). Hourly surges were computed as the difference between the observed and predicted (astronomical) tide values. Extreme surges were defined based on hourly values that exceeded the 99^{th} and separately 99.9^{th} percentiles of all surge hours from October through April over the period of record.

Hourly surge extremes, separated by less than 72 hours, were considered a single surge event. During each October –April season, these events were tallied producing series of surge counts for each tide station analogous to that for seasonal ECWS activity. Combining the unique surge events from the four stations also formed a regional extreme surge series. Unique station events were also required to be separated by at least 72 hours. It was rare that a regional event was based on an extreme from a single gauge. On average, 8.3 regional 99th percentile extreme surge events occurred in a season. While impacts did not necessarily occur with each of these events, the series provided an adequate number of events for subsequent analysis. Using the 99.9th percentile extremes, 1.4 regional surge events occurred on average in a season. This number is more in line with the frequency of moderate to severe ECWS impacts reported by Mather *et al.* (1964).

To relate the meteorological ECWS series to annual surge event counts, subsets of strong storms were developed based on different wind speed thresholds as well as various stronger pressure gradient criteria. Although the more stringent criteria reduced the number of storms classified as strong, the correlation among the series remained high, in most cases exceeding 0.90. Thus, the original (Hirsch *et al.* 2001) definition of strong storms, those with a maximum wind speed > 23.2 ms^{-1}, was retained for consistency. Hereafter this series is referred to as strong ECWS. When the strong storm series was compared to the series of regional 99th percentile surge occurrences (Figure 1), the series display modest correlation, with $r = 0.56$. For more extreme surges (99.9th percentile) only weak correlation is evident ($r = 0.23$).

Based on the 99th percentile, 13 of the 46 seasons (28%) experience 10 or more surge events (Table I). Given the season experiences 11 or more strong ECWS events, however, the likelihood of experiencing 10 or more 99th percentile surges more than doubles to 58% (Table I). This number of strong ECWS is observed in only 25% of the ECWS seasons. For the more extreme 99.9th percentile surges, two events can be expected in 32% of the years. In a year with ≥11 strong ECWS, there is a slightly higher than 42% chance that the season will experience two or more extreme surges (Table I). Collectively, Table I suggests that the ability to anticipate seasons in which ≥11 strong ECWS occur, maximizes the likelihood of experiencing a greater than average number of extreme surge events, regardless of whether surge events are defined by the 99th or 99.9th percentile.

Since the ability to anticipate active surge seasons directly would provide a more useful decision tool for emergency managers, the time series of regional 99th and 99.9th storm surge counts were substituted for the strong ECWS series in later analyses. A second, similar data set was also constructed in which the 99th or 99.9th surge events were required to occur in association with an ECWS. Hereafter these series are denoted ECWS-Surge. Using the 99.9th percentile threshold less than 7% of the surge hours were associated with meteorological events that were not classified as ECWS. Using the 99th percentile threshold, this figure increased to 24%. These cases were typically associated with storms that displayed westward movement as they traversed the coast or tracked through the Great Lakes to the west of the ECWS polygon. In many cases, a strong area of high pressure offshore accompanied the Great Lakes lows. This produced a strong pressure gradient along the east coast.

Overall the direct use of the storm surge data would provide the best characterization of seasons with high impact activity. However, since extreme surges can occur under a variety of meteorological conditions ranging from ECWS to strong high pressure systems, the direct use of the extreme surge series may result in suboptimal seasonal forecast skill. Presumably, the ability to forecast seasonal activity relies upon persistent atmospheric circulation features and hence a propensity for specific synoptic features such as ECWS. In such cases the enhanced ability to predict these features, which are most commonly associated with high surge events, may outweigh potentially less skillful forecast of surge events. Such forecasts are analogous to seasonal hurricane forecasts. These are currently followed closely by emergency managers in the study region, despite a relatively small increase in observed impacts during active hurricane seasons. The use of the third hybrid time series, reflecting only those surge events that occur in association with ECWS, as a basis for forecasting seasonal activity provides a compromise between the two extremes represented by the other time series.

2.2. Predictor variables

A set of eight predictor variables (Table II) was assembled based on analyses conducted by Hirsch *et al*. (2001). The first four predictors in Table II are global indices. Their inclusion accounts for the relationships between coastal storm frequency and SOI and Niño 3.4 SST anomalies identified by both Hirsch *et al*. (2001) and Noel and Changnon (1998); NAO-Atlantic storm track dependencies (e.g. Mailier *et al*., 2006); and the PDO (McCabe and Dettinger, 2002).

The remaining variables characterize sea and land surface temperatures within or adjacent to the ECWS quadrangle. Colucci (1976) and the conclusions of other researchers studying specific ECWS (e.g. Bosart 1981), point to land-sea temperature contrasts as contributing to the development and intensification of ECWS. Hoskins and Valdes (1990) also implicate such baroclinic regions as contributors to persistent Atlantic storm tracks.

Standardized anomalies were computed for each of these four local parameters. Gulf_SST encompassed the area from 29° N to 25°N and 83° W to 95°. SE_SST was defined over the area south of 35° N contained in the ECWS study region defined by Hirsch *et al*. (2001). SE_Land was computed based on area-weighted averages of U.S climate division values (Guttman and Quayle 1996) from the states of Florida, Georgia, South Carolina and North Carolina. For each month the difference between SE_Land and SE_SST was computed and standardized anomalies (Land-sea) computed from the set of differences.

3. Methods

3.1. Principal component analysis

To isolate the appropriate temporal averaging periods, DeGaetano *et al*., (2002) chose to prescreen a similar set of predictor variables, based on a suite of chi-squared tests. This approach compromised subsequent evaluation of the significance of the ECWS frequency predictions since the chi-squared procedure was not easily incorporated into the resampling procedures used for this purpose. As an alternative, a principal components analysis is used here to reduce the size of the original predictor pool. For each of the eight predictor variables, 3-month running averages were computed over the period from the October prior to the start of the ECWS season through April of the storm season. Hence, a set of 17 three-month averages was available for each of the 8 predictors. Of the 17 combined averages, 10 were purely predictive as none of the data was contained within the October to April storm period. Conversely, 7 averages were termed diagnostic in that they encompassed at least one month of the storm season. Separate PCA were conducted on these three data sets. Presentation of the resulting principal components equations is cumbersome given the large number of variables (e.g.

8 predictors x 7 averages for the smallest diagnostic data set). However the components can be reproduced based on the data sources from Table II and analysis with the software package R using the prcomp procedure (www.r-project.org).

Subjective principal component truncation criteria were used to select subsets of retained components. Although more rigorous component retention methods exist (Wilks, 2006), the resampling procedures used in the subsequent discriminant analyses assured that components representing only noise were not considered in formulating forecasts of seasonal storm activity. The retained components represent points on Figure 2 in which the eigenvalues associated with higher-order components stabilize. For reproducibility Table III summarizes the retained component subsets. Figure 3 summarizes these components in terms of the variables with the highest loadings.

3.2. Discriminant analysis

The retained component scores served as input to discriminant analyses. In the simplest case, storm and extreme surge counts were divided into two groups, segregating seasons with relatively high and low activity based on the quartiles or median of the 1959-2005 storm activity record. Storms were also segregated into three groups based on the terciles of the historical record. Table IV lists the boundaries of these groups for each of the four storm/surge definitions discussed in the previous subsection, the December – February storm counts (DJF ECWS) analyzed by DeGaetano *et al.* (2002), and counts of all ECWS meeting the criteria of Hirsch *et al.* (2001) including those which were present for only a single 6-hour period (All ECWS).

For these analyses, classification success was defined by the Kuiper skill score (KSS). This measure is given by the equation

$$KSS = \frac{ad - bc}{(a+c)(b+d)} \quad , \qquad (1)$$

where a is the number of events that occurred when forecasted, b is the number of times an event did not occur when forecasted, c is the number of events that occurred when not forecasted and d is the number of instances that an event was neither forecasted nor observed.

The KSS (Wilks, 2006) is a desirable measure of forecast skill since it treats random and constant (e.g. always forecasting below normal activity) forecasts equally, assigning them a score of zero. A perfect forecast is given a score of one. The KSS also assigns higher skill to a correct forecast when the alternative forecast is more likely.

A resampling procedure was used to determine the maximum number of dimensions to consider. Based on the original seasonal storm (surge) count time series, 10,000 bootstrap samples were generated (Wilks, 2006). For each randomized series, the combination of components yielding the maximum KSS was retained for each bootstrapped series. This resulted in an empirical distribution of KSS against which the original (non-bootstrapped) score could be compared. Discriminant functions were considered if the KSS exceeded the 90th percentile of the bootstrapped distribution. Bootstrapping in this manner is a feasible approach given the storm count series lack significant autocorrelation.

These analyses were conducted separately constraining the discriminant analysis to a fixed number of components. The one-dimensional case represents a point dividing the component time series into two storm-activity regions. More conventional 2- and 3-dimensional discriminant functions were also tested. The significance of the increase in

KSS resulting from the added dimensions was also assessed via resampling. Bootstrapped samples of KSS increase were generated by retaining the order of the original storm activity and lower dimension component series. The component series associated with the added dimension was randomized (10000 times) and the resulting KSS increase used to form a test distribution.

The classification success of the discriminant functions that displayed significant skill was re-evaluated based on leave-one-out cross-validation. The robustness of the discriminant functions was also evaluated by withholding non-overlapping sets of five years from the storm series, recomputing the functions based on the remaining n -5 year series, and assessing the success of these new functions in terms of their ability to classify the activity of the withheld years.

4. Results

4.1 Diagnostic components

Based on the set of diagnostic components (limited to the October through April ECWS season) seasons with ECWS activity within the upper quartile can be differentiated from lower activity seasons with significant skill (Figure 4). This was not the case for divisions based on the lower quartile or median, a result that was also reflected in the other storm and surge series (e.g. strong storms). Hence, hereafter the upper quartile will be used as the threshold dividing active from relatively inactive storm seasons.

Active All-ECWS seasons are typically associated with negative component 1 values and positive component 2 values (Figure 5a). Based on the component loadings

(Figure 3), this implies heightened ECWS activity occurs during seasons characterized by El Niño conditions and below-normal SST anomalies in the Gulf and along the Southeast coast. Although the skill of the three-dimensional discriminant analysis is also significant, consideration of a third component (component 4 in this case) only reassigns two seasons misclassified as active (circled symbols in Figure 5a). Component 4 reflects winter PDO conditions.

The components reflecting El Niño and PDO combine to produce statistically significant three-category classification success for All-ECWS activity. Like Figure 5a, the main difference between active and non-active seasons in Figure 5b, is the value of component 1, with active seasons characterized by generally negative values (i.e. El Niño). Component 4 (PDO) values tend to differentiate between seasons with normal and below-normal activity, with inactive seasons characterized by negative PDO index values.

The El Niño based component is no longer included when the strong ECWS data set is considered (Figure 5c). Rather, seasons with strong ECWS activity exceeding the 75^{th} percentile are characterized by below-normal winter SST anomalies in the Gulf and along the Southeast coast (positive component 2 values) and generally negative values of component 5. Based on the component loadings (Figure 3), this component implies that warmer SST in February, coupled with a low late autumn (October-November) land sea temperature contrast is conducive to strong storm activity.

In each of the panels in Figure 5, the 1982 ECWS season appears as an outlier. This season is associated with anomalously negative component 1 and component 2 scores. In addition to the occurrence of a strong El Niño event, this season was also preceded by the eruption of El Chichon in Mexico. It is possible the juxtaposition of these two climate anomalies influenced ECWS activity during this season. Elimination of this season had little effect on the results in Figure 5.

Based on the other definitions of storm activity, significant skill scores are not achieved for DJF ECWS or 99th percentile surge occurrences (Figure 4). Nonetheless, the highest skill for DJF ECWS is achieved using components 1 and 2. As was the case with the all ECWS series, high activity was generally observed in association with El Niño and below normal winter SST anomalies. This also agrees with DeGaetano *et al.* (2002) who found El Niño and Gulf and Southeast coastal SST as the best discriminant variables. For surge occurrence, component 2 is also included as a discriminant variable along with component 4 representing PDO conditions. The significant skill scores for the ECWS-surge series are based on the same components as the strong ECWS series.

4.2. Combined diagnostic components

4.2.1 *All-ECWS activity*

Based on the combined diagnostic components that span the period from the previous October through April of the ECWS season, similar results are obtained. For All-ECWS activity, the skills of the discriminant analyses decline and as a result are no longer significant (Figure 6). Nonetheless, the variables which give the highest skill reflect those which gave significant classification success in the within season analysis. Seasons with the highest activity are characterized by positive component 1 and 5 values which represent positive PDO values (and to some degree El Niño conditions) during and prior to the storm season as well as cooler than normal Gulf and land temperatures during the winter season. These results are in agreement with the diagnostic analysis, as these two components are the most highly correlated to the two components (1 and 2) that resulted in the best diagnostic skill (r= -0.85 and 0.74, respectively).

4.2.2. *Strong ECWS activity*

Unlike the ECWS activity in general, significant skill is obtained for the discrimination of seasons with high strong ECWS activity (Figure 6). Seasons with high storm activity tend to have negative values of both components 6 and 7 (Figure 7a). Here, active storm seasons are associated with warmer than normal SST in the Gulf during summer and but cooler land and sea surface temperature over the Southeast, during the spring prior to the ECWS season (Figure 3). Quantitatively, components 6 and 7 are most highly correlated with the two diagnostic components (components 2 and 5) that maximized strong ECWS classification skill (r= -0.36 and 0.41, respectively).

The anomalous 1982 season is the only high-activity season that is misclassified in Figure 7a. Excluding this year generally improves classification success, increasing the KSS from 56.5 to 68.9. However, the change in the discriminant function is minimal. In addition to the omission of the misclassified active season, two seasons with relatively low activity are reclassified to the correct group.

4.2.3. *Surge activity*

It is interesting to note that seasons with relatively few extreme surges (those in the lower 25^{th} percentile) can be distinguished from seasons with higher activity based on similar components (Figure 7b) that allow classification of the strong ECWS seasons (Figure 7a). The seasons with the lowest number of 99^{th} percentile surge events are characterized by positive component three values (Figure 7b). This represents cooler than normal SE_SST during the summer and fall preceding the ECWS season, in general agreement with the storm results that, based on component 6, indicate higher activity (and presumably more extreme surges) with warmer summer SST. The circled points in Figure 7b are reclassified when the third component (component 6) is considered.

4.3. Predictive components

4.3.1. *All-ECWS activity*

Based on predictive principal components (i.e. those based only on variables observed prior to the October – April ECWS season) the classification of All ECWS activity was similar to that based on variables observed during the ECWS season. Although the skill scores obtained for the predictive components were not significant based on the resampling procedures (Figure 8), the highest predictive classification success was achieved using components related to those that gave significant diagnostic classification success. High ECWS activity was associated with negative component 3 and positive component 5 values, indicating high storm activity following El Niño (positive PDO) summers.

4.3.1. *Strong ECWS activity*

Predictive components 4 and 6 resulted in the best classification of strong storm activity. (Figure 9a), The correlation between these two components and components 6 and 7 that were associated with significant classification success in the combined component analysis exceeded 0.85 Seasons with the highest activity are associated with generally negative component 4 and 6 values. This implies warm Gulf_SST anomalies during the preceding summer and cooler than normal temperatures in the Gulf and SE Coast during the previous late-winter and spring. The addition of a third variable (in this case component 5) resulted in only a modest increase in classification skill (KSS = 47.8). Component 5 represents El Niño conditions during the summer months. Although the classification of seven seasons changes when this third component is considered, in three cases correctly classified seasons become misclassified (Figure 9a).

The anomalous 1982 season is also problematic in Figure 9a. Omitting this season results in a small increase in KSS (from 43.5 to 46.7) and only a subtle change in the discriminant function. The increase in KSS results solely from the omission of 1982. Omitting 1982 had little effect on the classifications based on storm surge.

4.3.3. *Storm surge activity*

The predictive components also provided a means of classifying seasons with low 99th percentile surge activity (Figure 9b) using components 2 and 4. These components are most highly correlated with combined components 3 and 6, (r = 0.60 and 0.87, respectively) two of the three components that gave significant classification skill. Seasons with low surge activity were typically characterized by positive component 2 values, representing colder than average SST in the Gulf and SE Coastal regions during the prior winter.

4.4. Predictive cross validation

Figure 10 illustrates the ability of the predictive components to classify seasonal storm and surge activity using independent data. These results are based on the cross validation analyses with non-overlapping five year periods omitted. Similar results are obtained for leave-one-out cross validation. For the independent strong storm counts and surge occurrences, KSS decreases only slightly from 43.4 using the dependent sample to 42.2 in both cases. For storm activity, 10 of the 12 (83%) seasons with activity in the upper quartile are assigned to the correct category (Figure 10a). Of the remaining 34 seasons, 65% are correctly classified (Figure 10a). From a practical standpoint, given a forecast of strong storm activity in the lower three-quartile category, in only 8% of the cases was higher ECWS activity observed. Conversely, a forecast of strong ECWS activity in the upper quartile results in a high number of false alarms, as the subsequent number of ECWS will fall within this range only 45% of the time. This is not surprising given the distribution of points in the high activity sector of Figure 9a. Nonetheless, the probability of high ECWS given such a forecast is much higher than expected with no *a priori* knowledge.

For storm surge activity (Figure 10b), 9 of the 12 seasons (75%) with surge activity in the lower quartile are assigned to the correct category. Of the remaining 34 seasons, 71% are correctly classified (Figure 10b). Given a forecast of surge activity in the upper-three-quartile category, in only 11% of the cases was lower surge activity observed. If a forecast of surge activity within the lower quartile is indicated, activity in this range is realized in only 47% of the cases. Like forecasts of high ECWS activity, despite the high number of false alarms, such forecasts do imply a higher than expected probability (i.e. 25%) that a particular season will have relatively few extreme surge events. It should also be noted that since 1981, the false alarm rate for low surge activity forecasts decreases to 25%. It is unclear whether this is a natural artifact of the surge series, or if non-climatological influences bias the pre-1981 data record. Three of the four tide gauges were relocated in 1989. Although the data were adjusted for the 1983 change in epoch, it is unclear whether this adjustment also factored in the relocation of the gauge. The simultaneous relocation of the gauges and low correlation between surge series from other nearby gauges precluded a more formal analysis of the homogeneity of the surge series.

In terms of the diagnostic component data sets cross validated skill is comparable, despite reliance on observations from within the ECWS season. Using the combined components for strong ECWS, all but one of the seasons (1982) in which activity in the lower 3 quartiles is forecasted experiences activity within the upper quartile (Figure 10a). For storm surge, the cross validated skill based on the combined components also remains high. The combined components tend to improve classification success in the earlier part of the record, but at the expense of correct classification in the post 1981 period (Figure 10b).

5. Summary

Collectively, the results presented here, although similar to DeGaetano *et al.* (2002) are more robust. The use of principal component analysis to reduce the initial intercorrelated pool of discriminant variables and refined statistical analyses highlight two features that were obscured by the various, mostly non-significant, relationships presented in the original work. From a meteorological perspective, it is primarily El Niño phase, with some influence from PDO phase, that characterizes active ECWS seasons. Cooler-than-normal Gulf_SST and SE_SST during the storm seasons also correspond to heightened activity. DeGaetano *et al.* (2001) show positive correlation ($r = 0.45$) between these temperatures and NAO phase.

El Niño, however, has little relationship to the prevalence of stronger storms and the potential for storm impacts along New York's Long Island. Here, SST, both in the

Gulf and off the Southeast coast, exert the greatest influence. An increased frequency of strong storms can be anticipated when warmer-than-normal SST characterize these regions during the summer months preceding the ECWS season.

In terms of extreme surge activity, significant KSS could not be obtained. However, the relationships associated with the highest KSS reinforced the significant results noted for strong storm activity. Most notably, decreased surge activity tends to follow summers in which Gulf_SST and SE_SST are below normal. From a practical standpoint, it is unfortunate that seasons in which the most extreme 99.9th percentile surge events occur cannot be forecast with significant skill, as such information would be the most beneficial to coastal interests.

Although the strong storm and surge series are related, a notable difference is that the storms represent coast-wide conditions as they can be located within the relatively large polygon defined by Hirsch *et al*. (2001) that extends from 45° to 30° latitude along the East Coast. The extreme surges, however, are affected by storms that traverse only a limited part of this region. This limitation, acts to diminish the seasonal predictability as synoptic and smaller scale factors, specific to individual storm events, govern the presence and magnitude of storm surge. Thus, while the ability to anticipate regional seasonal storm activity based larger scale conditions exists, the factors that govern the nuances of individual storms at specific locations are less predictable on a seasonal basis.

Nonetheless, much like seasonal hurricane forecasts, which offer limited insight into the associated impacts along a specific stretch of coast, these seasonal ECWS relationships have practical seasonal forecast applications for coastal interests in the metropolitan Northeast. Given SST data observed prior to the start of the October storm season, subsequent storm activity and to some degree tidal impacts can be anticipated. Given that above-normal summer SST conditions are preceded by cooler-than-normal land and sea surface temperatures in (and adjacent to) the Southeastern U.S. there is an only 10% chance that an active strong ECWS season will follow. In terms of storm surge activity, warmer-than-normal SST in the Gulf and off the Southeast Coast during the previous winter indicate that an active surge season is unlikely to follow. Such relationships provide useful information to emergency managers and coastal engineers in terms of decisions related to budget and project management and public preparedness. Although forecasts for above normal storm activity (below normal surge activity) are associated with high false alarm rates, in a probabilistic sense these forecasts also provide some useful guidance. Using storm activity as an example, in any given year there is a 25% chance of experiencing activity in the upper quartile. Given a forecast of above normal activity, this probability nearly doubles to 45%.

6. Acknowledgments

This work was supported by NOAA Grant NA05OAR4311122 as part of the Transition of Research Applications to Climate Services (TRACS) program. Partial support from NOAA Contract EA133E-02-CN-0033 and NSF grant ATM-0531817 is also acknowledged.

7. References

Bosart LF. 1981. The President's Day snowstorm of 18-19 February 1979: A subsynoptic-scale event. *Monthly Weather Review* **109**: 1542-1566.

Chan AC, Colucci SJ, DeGaetano AT. 2003. Predicting east coast winter storm frequencies from midtropospheric geopotential height patterns. *Weather and Forecasting* **18**: 1177–1191.

Colucci SJ. 1976. Winter cyclone frequencies over the eastern United States and adjacent western Atlantic. 1964-1973 *Bulletin of the American Meteorological Society* **57**: 548-553.

Davis RE, Dolan R, Demme G. 1993. Synoptic climatology of Atlantic coast northeasters. *International Journal of Climatology* **13**: 171-189.

DeGaetano AT, Hirsch ME, Colucci SJ. 2002. Statistical prediction of seasonal East Coast winter storm frequency. *Journal of Climate* **15**: 1101-1117.

Guttman NB, Quayle RG. 1996. A historical perspective of U.S. climate divisions. *Bulletin of the American Meteorological Society* **77**: 293-303.

Hess KW. 2003. Puget Sound tidal datums by spatial interpolation. *In*: Proceedings of the American Meteorological Society Fifth Conference on Coastal Atmospheric and Oceanic Prediction and Processes, Seattle, WA.

Hoskins BJ, Valdes PJ. 1990. On the existence of storm tracks. *Journal of Atmospheric Science* **47**: 1854-1864.

Hirsch ME, DeGaetano AT, Colucci SJ. 2001. An east coast winter storm climatology. *Journal Climate* **14**: 882-899.

Kalnay E, [and Co-authors]. 1996. The NCEP/NCAR 40-Year Reanalysis Project. *Bulletin of the American Meteorological Society* **77**: 437-471.

Leatherman SP. 1982. *Barrier Island Handbook*. University of Maryland Press: College Park, MD, USA.

Mather JR, Adams III H, Yoshioka GA. 1964. Coastal storms of the eastern United States. *Journal of Applied Meteorology* **3**: 693-706.

Mailier PJ, Stephenson DB, Ferro CAT, Hodges KI. 2006. Serial clustering of extratropical cyclones. *Monthly Weather Review* **134**: 2224–2240.

McCabe GJ, Dettinger MD. 2002. Primary models of predictability of year-to-year snowpack variations in the western United States from teleconnections with Pacific Ocean climate. *Journal of Hydrometeorol*ogy **3**: 13-25.

Noel J, Changnon D. 1998. A pilot study examining U.S. winter cyclone frequency patterns associated with three ENSO parameters. *Journal of Climate* **11**: 2152-2159.

Wilks DS. 2006. *Statistical Methods in the Atmospheric Sciences 2nd Ed.* Academic Press: San Diego, CA, USA.

Table Legends

Table I. Percentage of seasons with greater than or equal to the number of surge events. The percentage of high surge events occurring during seasons with the specified numbers of ECWS events is also given.

Table II. Variables used to predict seasonal ECWS frequencies.

Table III. Number of retained components and cumulative explained variance for principal component subsets.

Table IV. Thresholds used to define seasons with relatively high and low storm activity.

Table I. Percentage of seasons with greater than or equal to the number of surge events. The percentage of high surge events occurring during seasons with the specified numbers of ECWS events is also given.

Number of	Percent of	Percent of Surge Events Occurring in Seasons with			
Surge Events	all Seasons	≥12 ECWS	≥11 ECWS	≥10 ECWS	≥9 ECWS
14	2	13	8	5	4
13	9	13	17	20	16
12	11	25	25	25	20
11	17	25	33	30	24
10	28	25	58	45	40
9	28	25	58	45	40
8	40	38	75	65	56
3*	13	13	17	10	16
2*	32	25	42	40	44
1*	66	25	67	75	72

* surge events based on the 99.9^{th} percentile.

Table II. Variables used to predict seasonal ECWS frequencies.

Variable	Abbreviation	Data Source
Niño 3.4 SST Anomaly	Niño 3.4	<http://www.cpc.ncep.noaa.gov/data/indices/sstoi.indices>
Southern Oscillation Index	SOI	< http://www.cpc.ncep.noaa.gov/data/indices/soi >
North Atlantic Oscillation Index	NAO	< http://www.tiempocyberclimate.org/portal/datanao.htm >
Pacific Decadal Oscillation Index	PDO	< http://jisao.washington.edu/pdo/PDO.latest >
Gulf of Mexico SST anomaly	GULF_SST	NCAR/NCEP Reanalysis Data Set
Southeast Coastal SST Anomaly	SE_SST	NCAR/NCEP Reanalysis Data Set
Southeast Land Temp. Anomaly	SE_Land	U.S. Climate Division Data
SE Land – SE SST Anomaly	Land-sea	Reanalysis and Climate Division Data

Table III. Number of retained components and cumulative explained variance for principal component subsets.

Component Set	Months	Number of Retained Components	Cumulative Explained Variance (%)
Predictive	Oct_{-1} – Sep	7	82
Diagnostic	Oct. – Apr	5	89
Combined	Oct_{-1} – Apr	7	77

* -1 denotes the year prior to ECWS season commencement.

Table IV. Thresholds used to define seasons with relatively high and low storm activity.

Storm Set	Percentile Threshold* 25	50	75	terciles
All ECWS	21	23	26	22 24
Strong ECWS	6	9	11	7 9
DJF ECWS	5	8	10	7 8
Regional 99th Surge	4	6	10	4 7
Regional 99.9th Surge	0	1	2	1 1
ECWS-99th Surge	2	4	6	3 5

* Using the 25th percentile, seasons with the number of listed storms or fewer define inactive seasons. For the 50th and 75th percentiles active seasons have the listed number or more storms. Using the tercile thresholds, inactive (active) seasons have fewer (more) storms than the first (last) listed value.

Figure Captions

Figure 1. Annual number of strong ECWS (solid line with closed circles), 99^{th} percentile (dotted line with closed circles) and 99.9^{th} percentile (solid line with open circles) regional surge events.

Figure 2. Eigenvalue magnitudes as a function of principal component number for the predictive (solid squares); diagnostic (solid circles) and combined (open circles) sets of principal components.

Figure 3. Variables with the five highest loadings in the diagnostic (top grid, right of thick line), predictive (top grid, left of thick line) and combined (bottom grid) principal component subsets. Rows represent variables (Table II) and columns the starting month used to compute three-month averages of the corresponding variable. Months are denoted numerically with a minus sign used in the year prior to the storm season and a plus sign used for months in the subsequent year. The number within each grid is the component number with negative signs used to denote the sign of the loading.

Figure 4. Skill score associated with 1, 2, and 3 variable (diagnostic component) discriminant analyses (from left to right respectively in each grouping of bars) for different definitions of seasonal storm activity. The number in each bar represents the probability of achieving the plotted skill score by chance. Bars showing significant skill ($p > 0.10$) are shaded.

Figure 5. Linear discriminant analysis results for a) upper quartile grouping of the All-ECWS data set, b) tercile grouping of the All-ECWS data set and c) upper quartile grouping of the strong ECWS data set based on diagnostic principal components. Seasons with the highest activity are denoted as solid circles. The gray squares show seasons with the lowest activity in panel b. Circled symbols represent cases that are reclassified when an additional variable is considered.

Figure 6. As in Figure 4, but based on the combined diagnostic set of component scores.

Figure 7. As in Figure 5c except for the combined diagnostic set of components for a) strong ECWS and b) 99^{th} percentile surge events. In panel b open squares denote seasons with surge occurrence in the lower quartile.

Figure 8. Skill score associated with 1, 2, and 3 variable (predictive component) discriminant analyses (from left to right respectively in each grouping of bars) for different definitions of seasonal storm activity.

Figure 9. As in Figure 7 except for the predictive set of components.

Figure 10. Cross validation results omitting non-overlapping 5-year periods. Dots indicate observed a) strong ECWS and b) 99th percentile surge events. Gray bars show the category indicated by the predictive component discriminant functions. White bars show cross validation results using the combined component discriminant functions.

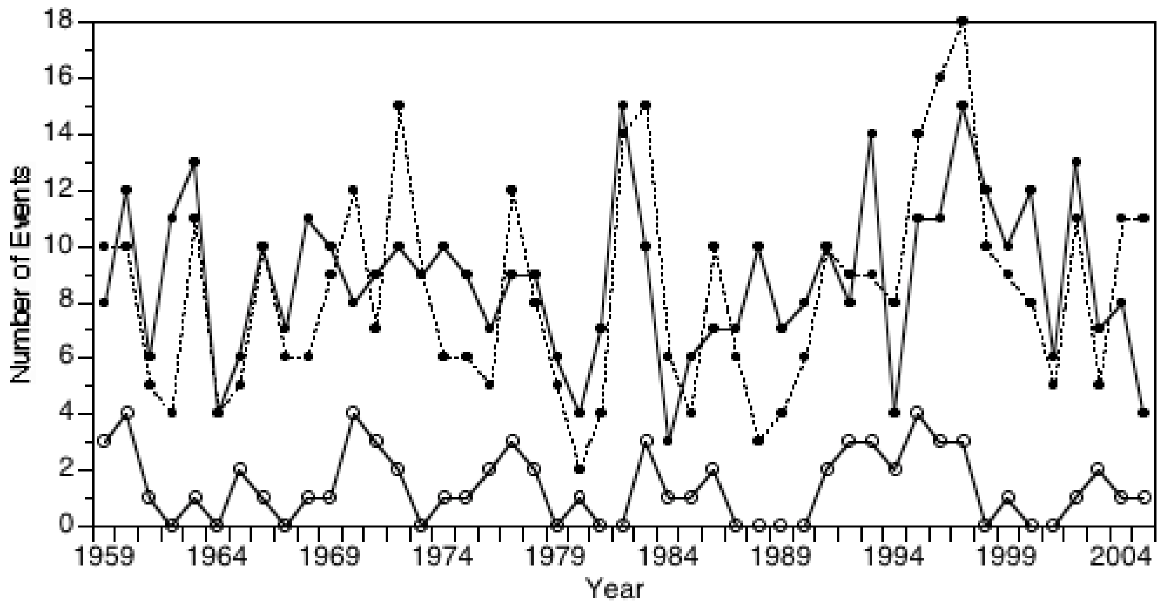

Figure 1. Annual number of strong ECWS (solid line with closed circles), 99th percentile (dotted line with closed circles) and 99.9th percentile (solid line with open circles) regional surge events.

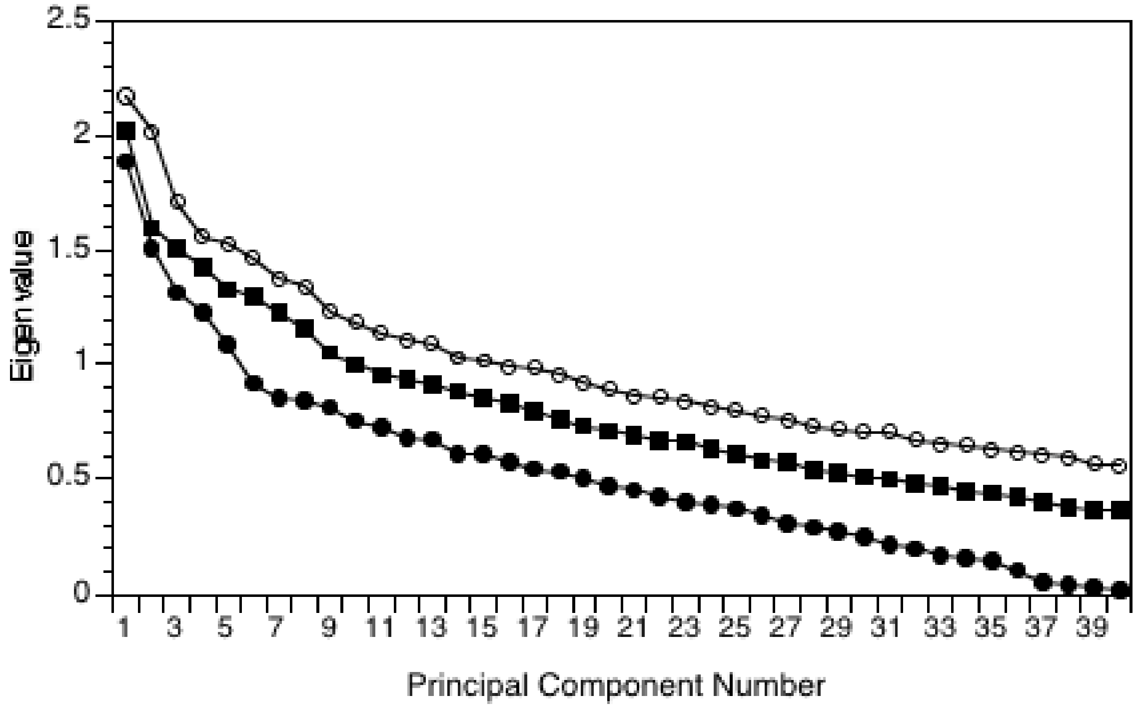

Figure 2. Eigenvalue magnitudes as a function of principal component number for the predictive (solid squares); diagnostic (solid circles) and combined (open circles) sets of principal components.

Variable	-10	-11	-12	1	2	3	4	5	6	7	8	9	10	11	12	+1	+2
SOI		-1	-1	-1				-5	3 / -5	3 / -5				1	1	1	
Nino3.4	1	1							5	5			-1	-1			
NAO										6					-3	-3	-3
Gulf_SST		-2	-2	-2			-4	-4	-4	-4 / -6				-2	-2		-5
SE_SST	7	4	-2	-2	6	6							4	-2	-2	-2	-5
SE_Land																-3	
Land-Sea					6								5	5		-3	-5
PDO	7	7	7	7				-3	-3	-3			4	4	4	4	

Variable	-10	-11	-12	1	2	3	4	5	6	7	8	9	10	11	12	+1	+2
SOI		2	2	2													
Nino3.4	-2	-2												1			
NAO			-4											-5	-5		
Gulf_SST			-4			7		-6	-6	-6	-3				-5		
SE_SST	6		-4		7	7				-3	-3	-3	-3	6			
SE_Land		-4	-4		7	7								-5	-5		
Land-Sea																	
PDO									1	1						1	1

Figure 3. Variables with the five highest loadings in the diagnostic (top grid, right of thick line), predictive (top grid, left of thick line) and combined (bottom grid) principal component subsets. Rows represent variables (Table II) and columns the starting month used to compute three-month averages of the corresponding variable. Months are denoted numerically with a minus sign used in the year prior to the storm season and a plus sign used for months in the subsequent year. The number within each grid is the component number with negative signs used to denote the sign of the loading.

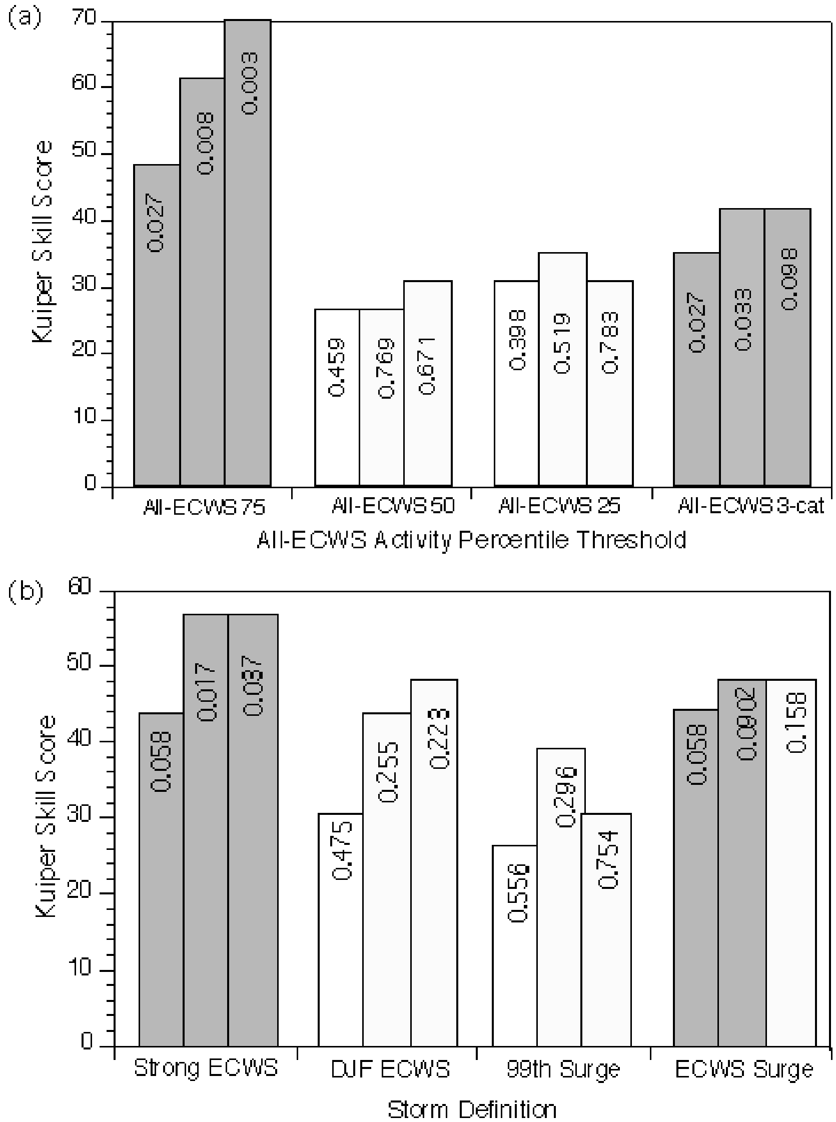

Figure 4. Skill score associated with 1, 2, and 3 variable (diagnostic component) discriminant analyses (from left to right respectively in each grouping of bars) for different definitions of seasonal storm activity. The number in each bar represents the probability of achieving the plotted skill score by chance. Bars showing significant skill (p > 0.10) are shaded.

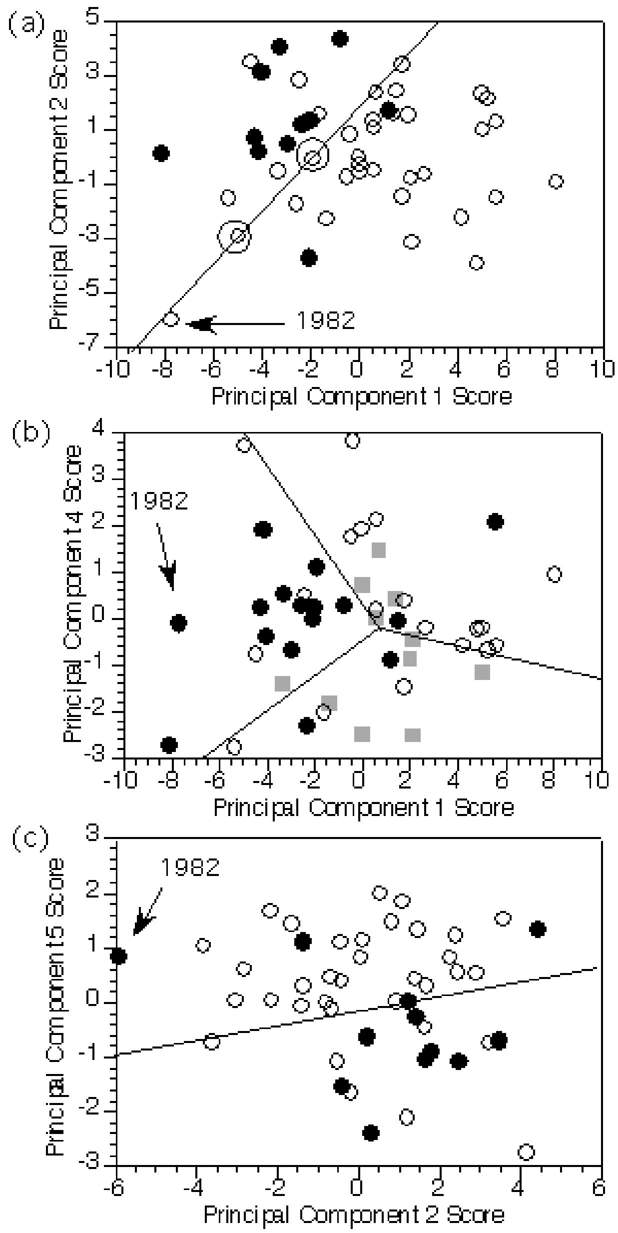

Figure 5. Linear discriminant analysis results for a) upper quartile grouping of the All-ECWS data set, b) tercile grouping of the All-ECWS data set and c) upper quartile grouping of the strong ECWS data set based on diagnostic principal components. Seasons with the highest activity are denoted as solid circles. The gray squares show seasons with the lowest activity in panel b. Circled symbols represent cases that are reclassified when an additional variable is considered.

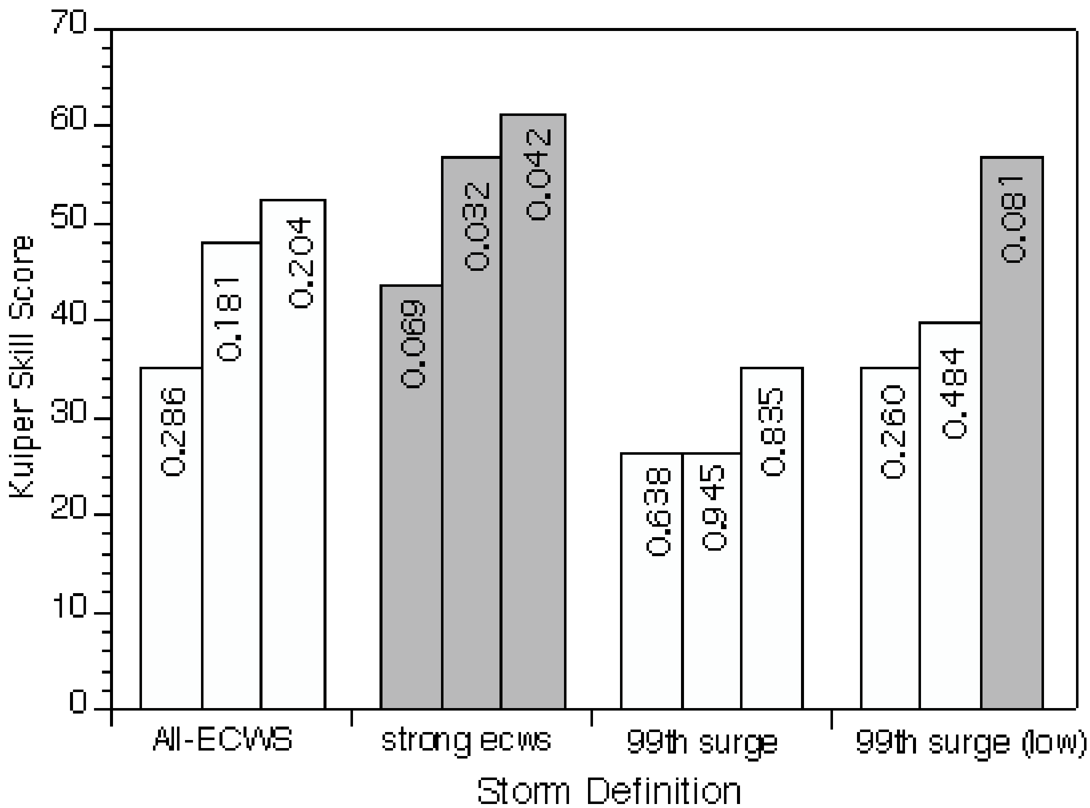

Figure 6. As in Figure 4, but based on the combined diagnostic set of component scores.

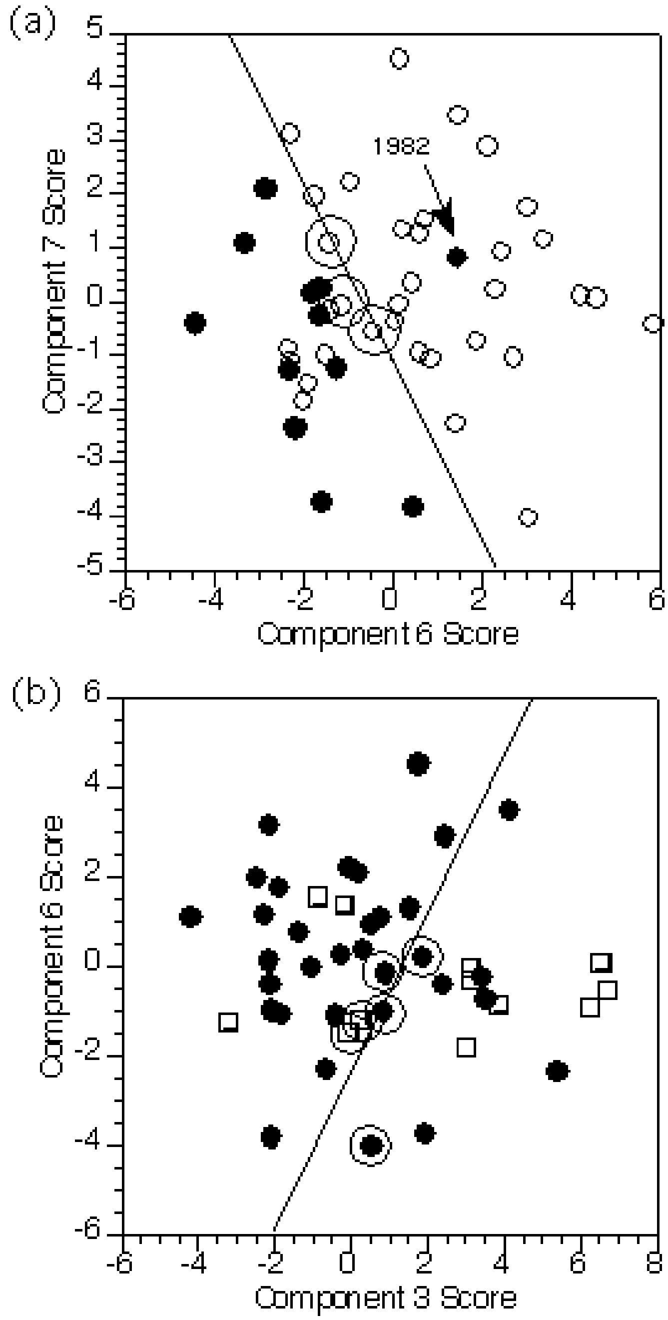

Figure 7. As in Figure 5c except for the combined diagnostic set of components for a) strong ECWS and b) 99th percentile surge events. In panel b open squares denote seasons with surge occurrence in the lower quartile.

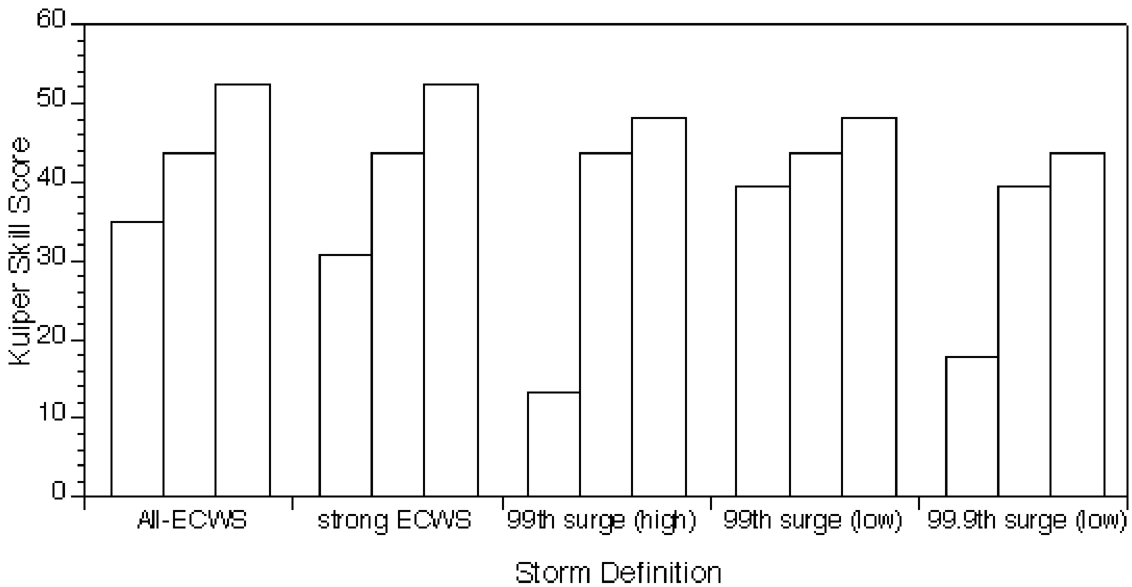

Figure 8. Skill score associated with 1, 2, and 3 variable (predictive component) discriminate analyses (from left to right respectively in each grouping of bars) for different definitions of seasonal storm activity.

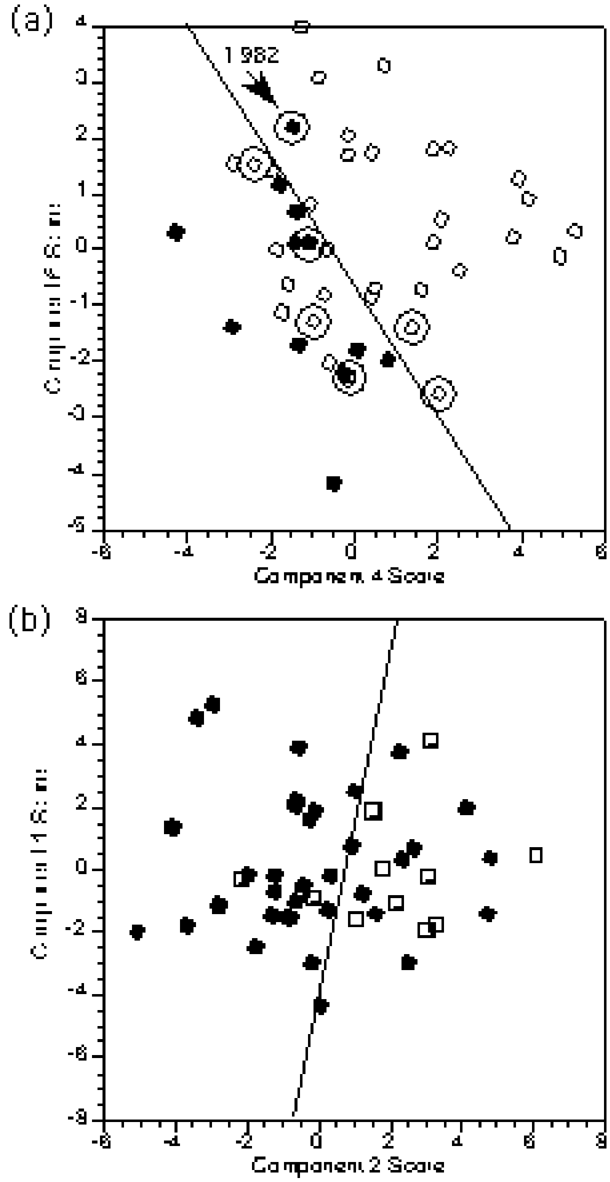

Figure 9 As in Figure 7 except for the predictive set of components.

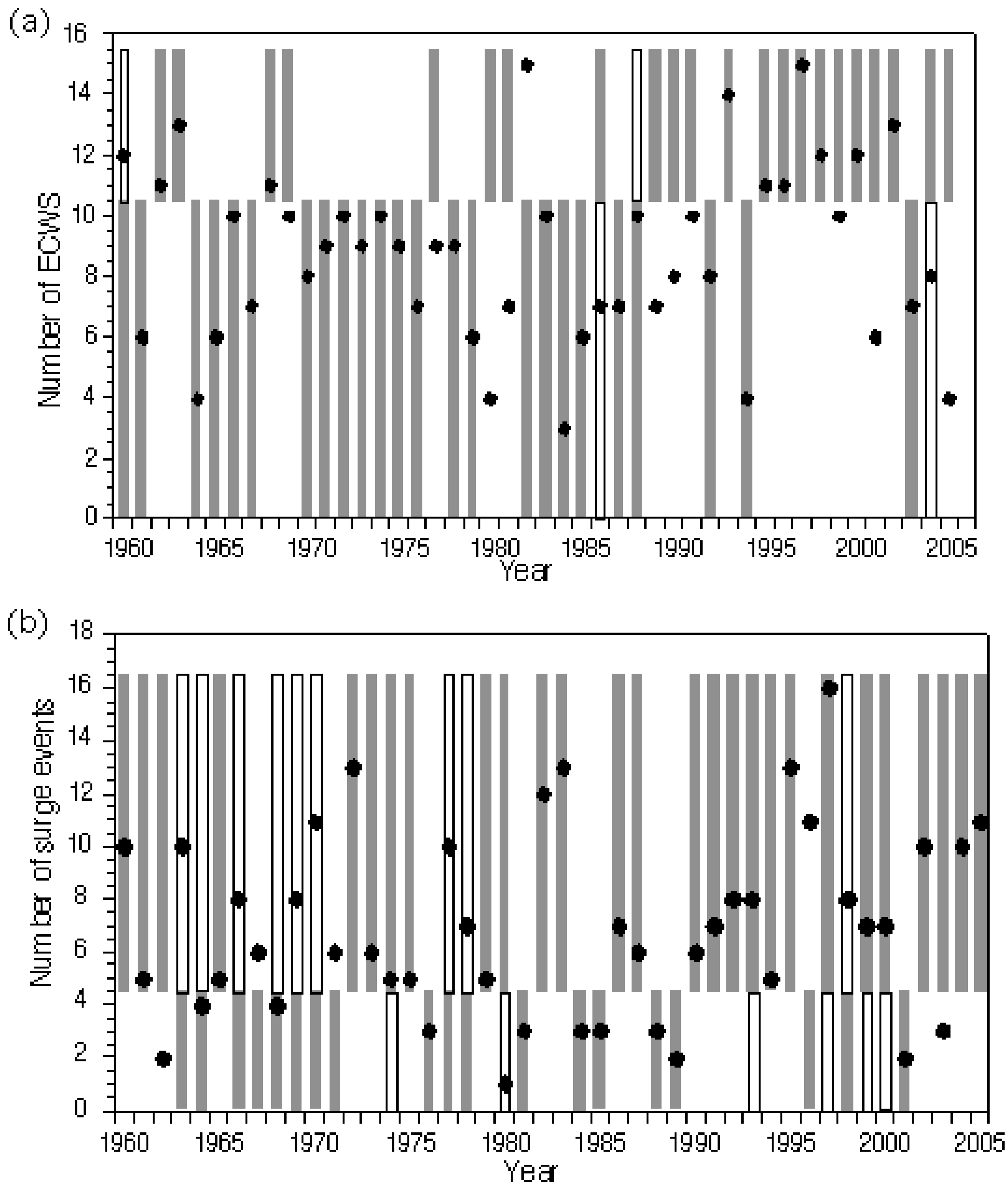

Figure 10. Cross validation results omitting non-overlapping 5-year periods. Dots indicate observed a) strong ECWS and b) 99th percentile surge events. Gray bars show the category indicated by the predictive component discriminant functions. White bars show cross validation results using the combined component discriminant functions.